Quantum Squeezing Induced Optical Nonreciprocity

Lei Tang,[1] Jiangshan Tang,[1] Mingyuan Chen,[1] Franco Nori,[2,3] Min Xiao,[1,4] and Keyu Xia[1,5,*]

[1]*College of Engineering and Applied Sciences, National Laboratory of Solid State Microstructures, and Collaborative Innovation Center of Advanced Microstructures, Nanjing University, Nanjing 210093, China*

[2]*RIKEN Quantum Computing Center, RIKEN Cluster for Pioneering Research, Wako-shi, Saitama 351-0198, Japan*

[3]*Physics Department, The University of Michigan, Ann Arbor, Michigan 48109-1040, USA*

[4]*Department of Physics, University of Arkansas, Fayetteville, Arkansas 72701, USA*

[5]*Jiangsu Key Laboratory of Artificial Functional Materials, Nanjing University, Nanjing 210023, China*

(Received 12 October 2021; accepted 12 January 2022; published 23 February 2022)

We propose an all-optical approach to achieve optical nonreciprocity on a chip by quantum squeezing one of two coupled resonator modes. By parametric pumping a $\chi^{(2)}$-nonlinear resonator unidirectionally with *a classical coherent field*, we squeeze the resonator mode in a selective direction due to the phase-matching condition, and induce a chiral photon interaction between two resonators. Based on this chiral interresonator coupling, we achieve an all-optical diode and a three-port quasicirculator. By applying *a second squeezed-vacuum field* to the squeezed resonator mode, our nonreciprocal device also works for single-photon pulses. We obtain an isolation ratio of > 40 dB for the diode and fidelity of $> 98\%$ for the quasicirculator, and insertion loss of < 1 dB for both. We also show that nonreciprocal transmission of strong light can be switched on and off by a relative weak pump light. This achievement implies *a nonreciprocal optical transistor*. Our protocol opens up a new route to achieve integrable all-optical nonreciprocal devices permitting chip-compatible optical isolation and nonreciporcal quantum information processing.

DOI: 10.1103/PhysRevLett.128.083604

Optical nonreciprocal devices, such as optical diodes and circulators, can separate backscattering signals from a light source. The conventional magneto-optical approach to achieve optical nonreciprocity (ONR) is difficult to integrate on a chip because it requires strong magnetic fields and bulky materials [1,2]. Developing a new mechanism for magnetic-free ONR is of interest in fundamental physics and promises important applications for on-chip light manipulation. Various magnetic-free optical nonreciprocal devices have been theoretically proposed and experimentally demonstrated by exploiting optical nonlinearities [3–11], spatiotemporal modulation of the medium [12–14], spin-momentum locking in chiral quantum optical systems [15–23], directional optomechanical coupling [24–26], moving atomic lattices [27–29], atomic reservoir engineering [30], the Sagnac effect in spinning resonators [31–33], and susceptiblity-momentum locking in atomic gases [34–40]. Kerr-nonlinear optical nonreciprocal devices are compatible with a chip, but subject to dynamic reciprocity [6]. Despite many efforts, it is challenging to realize a chip-compatible all-optical nonreciprocal device without moving parts or spatiotemporal modulation. By directionally amplifying the single-photon interaction in a $\chi^{(2)}$ microring resonator via the mode mean field, one can induce chiral normal mode splitting (NMS) and construct on-chip optical isolators [41]. Nevertheless, the demanded three-mode phase matching in one resonator is a significant challenge [42], and normally leads to an inefficient detuned driving, resulting in a weak ONR and a large insertion loss [41].

Quantum squeezing of a $\chi^{(2)}$ resonator mode can exponentially amplify the interaction between quantum objects. It could solve various challenging tasks [43–52]. Nevertheless, it is still an open question how to achieve ONR via quantum squeezing. Here, we show that high-performance ONR can be achieved by directionally squeezing the resonator mode with a *coherent* laser field. With this chiral quantum squeezing, we achieve an optical diode, a quasicirculator and, for the first time, a nonreciprocal optical transistor. Note that our method is based on directional quantum squeezing and thus conceptually differs from Ref. [41]. Our method only needs two-mode matching in one resonator and thus greatly simplifies its experimental implementation.

The schematic of our proposed system is depicted in Fig. 1. It consists of two coupled whispering-gallery mode microring resonators and two nearby optical waveguides. The resonators can be made of high-quality thin film with $\chi^{(2)}$ nonlinearity, e.g., lithium niobate or aluminum nitride. Thus, the resonators support the parametric nonlinear optical process. The resonator B (R_B) is pumped from port 3 by a continuous wave coherent laser field with frequency ω_p, amplitude α_p, and phase θ_p. This *classical* pump generates a squeezing interaction with strength Ω_p for the counterclockwise (CCW) mode $b_{\circlearrowleft}$. Because of the

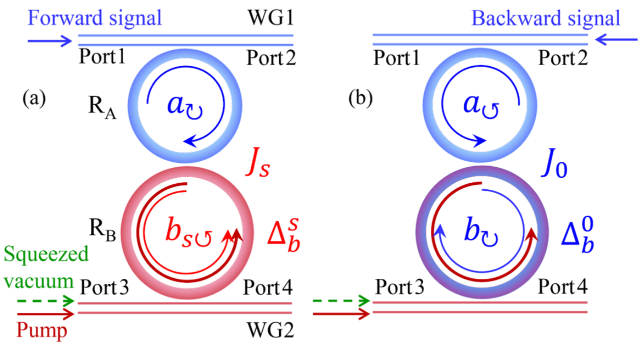

FIG. 1. Schematic of an all-optical nonreciprocal system consisting of two microring resonators (R_A and R_B) and two nearby optical waveguides (WG1 and WG2). To achieve *classical light isolation*, a coherent pump field is applied to generate a CCW squeezing mode $b_{s\circlearrowleft}$ in R_B. To achieve *single-photon isolation*, a broadband squeezed-vacuum field is used to drive R_B. (a) A forward-input signal field excites a CW mode $a_\circlearrowright$ in R_A, which interacts with the squeezed mode $b_{s\circlearrowleft}$ with a coupling rate J_s. (b) A backward-input signal field stimulates a CCW mode $a_\circlearrowleft$ in R_A. It couples to a CW bare mode $b_\circlearrowright$ in R_B with a bare coupling rate J_0.

directional phase-matching condition in the parametric nonlinear process, the mode $b_\circlearrowleft$ is squeezed to a mode $b_{s\circlearrowleft}$, but the clockwise (CW) mode $b_\circlearrowright$ is unsqueezed. The resonator A (R_A) slightly differs in size from R_B, such that the pump field cannot drive the parametric nonlinear process in the former. In this arrangement, we only need to consider mode squeezing in R_B.

Now we discuss how the pump laser modulates the inter-resonator interaction and causes the ONR. In the forward-input case, a signal field input to port 1 excites the CW mode $a_\circlearrowright$ in R_A. Because of the pump field, the mode $a_\circlearrowright$ couples to the squeezed mode $b_{s\circlearrowleft}$ with a rate J_s. The pump also causes a frequency shift to $b_{s\circlearrowleft}$ with respect to the bare mode $b_\circlearrowleft$. In comparison, in the backward-input case, a signal field from port 2 excites the CCW mode $a_\circlearrowleft$ in R_A. In this case, the pump field has no action on the CW mode $b_\circlearrowright$. This case is equivalent to the unpumped system only consisting of two coupled resonators. Thus, the mode $a_\circlearrowleft$ interacts with the bare mode $b_\circlearrowright$ with a unmodulated coupling rate J_0.

In the frame rotating at frequency $\omega_p/2$, the Hamiltonian for the forward-input case reads

$$\begin{aligned}
&\mathcal{H}_{\rm fw} = \mathcal{H}_A + \mathcal{H}_B + \mathcal{H}_J,\\
&\mathcal{H}_A/\hbar = \Delta_p^a a_\circlearrowright^\dagger a_\circlearrowright + i\sqrt{2\kappa_{\rm ex1}}(a_{\rm in} a_\circlearrowright^\dagger e^{-i\Delta_{\rm in}t} - a_{\rm in}^\dagger a_\circlearrowright e^{i\Delta_{\rm in}t}),\\
&\mathcal{H}_B/\hbar = \Delta_p^b b_\circlearrowleft^\dagger b_\circlearrowleft + \Omega_p(e^{-i\theta_p} b_\circlearrowleft^{\dagger 2} + e^{i\theta_p} b_\circlearrowleft^2)/2,\\
&\mathcal{H}_J/\hbar = J_0(a_\circlearrowright^\dagger b_\circlearrowleft + a_\circlearrowright b_\circlearrowleft^\dagger), \qquad (1)
\end{aligned}$$

where the detunings are $\Delta_p^{a/b} = \omega_{a/b} - \omega_p/2$ and $\Delta_{\rm in} = \omega_{\rm in} - \omega_p/2$, $\omega_{a/b}$ is the resonance frequency of $R_{A/B}$, $\omega_{\rm in}$ is the frequency of the signal mode $a_{\rm in}$, and $\kappa_{\rm ex1}$ is the external decay rate of R_A. The pump strength Ω_p is created by driving a mode $c_\circlearrowleft$ of R_B with an external field α_p. It is determined by the pump laser power P_p (see Supplemental Material [53] for the detailed derivation and relation of Ω_p and P_p).

Applying the Bogoliubov squeezing transformation [43,44,56,57] $b_s = \cosh(r_p)b + e^{-i\theta_p}\sinh(r_p)b^\dagger$ with the squeezing parameter $r_p = \frac{1}{4}\ln[(1+\beta)/(1-\beta)]$ and $\beta = \Omega_p/\Delta_p^b$, we can transform the Hamiltonian $\mathcal{H}_{\rm fw}$ to the squeezing picture. We further apply the rotating-wave approximation $\Delta_p^a + \Delta_p^b\sqrt{1-\beta^2} \gg \sinh(r_p)J_0$ in the squeezing picture and neglect the counterrotating terms. Then, the Hamiltonian in the frame rotating at frequency of $\Delta_{\rm in}$ becomes $\mathcal{H}_{\rm fw}^s/\hbar = \Delta_a a_\circlearrowright^\dagger a_\circlearrowright + i\sqrt{2\kappa_{\rm ex1}}(a_{\rm in}a_\circlearrowright^\dagger - a_{\rm in}^\dagger a_\circlearrowright) + \Delta_b^s b_{s\circlearrowleft}^\dagger b_{s\circlearrowleft} + J_s(a_\circlearrowright^\dagger b_{s\circlearrowleft} + b_{s\circlearrowleft}^\dagger a_\circlearrowright)$, where $\Delta_a = \omega_a - \omega_{\rm in}$, $\Delta_b^s = \Delta_p^{bs} - \Delta_{\rm in}$, $\Delta_p^{bs} = \Delta_p^b\sqrt{1-\beta^2}$ and $J_s = \cosh(r_p)J_0$. The effective squeezed mode detuning Δ_b^s and the effective coupling rate J_s are controlled by the pump field Ω_p and the corresponding detuning Δ_p^b. When the ratio β approaches unity, the rate J_s between $a_\circlearrowright$ and $b_{s\circlearrowleft}$ is enhanced exponentially with respect to the rate J_0 [53].

In the squeezing picture, the master equation of the system without a squeezed-vacuum driving takes the form $d\rho_{\rm fw}/dt = -i[\mathcal{H}_{\rm fw}^s, \rho_{\rm fw}] + (\mathcal{L}[L_a] + \mathcal{L}[L_{bs}] + \pounds_n[L_{bs}])\rho_{\rm fw}$, where $\rho_{\rm fw}$ is the system density matrix, the term $\mathcal{L}[L_a]\rho_{\rm fw}$ ($\mathcal{L}[L_{bs}]\rho_{\rm fw}$) with operator $L_a = \sqrt{\kappa_a}a_\circlearrowright$ ($L_{bs} = \sqrt{\kappa_b}b_{s\circlearrowleft}$) describes the decay of the mode $a_\circlearrowright$ ($b_{s\circlearrowleft}$) with a rate κ_a (κ_b), and $\mathcal{L}[o]\rho = 2o\rho o^\dagger - o^\dagger o\rho - \rho o^\dagger o$. Here, $\kappa_a = \kappa_{\rm ex1} + \kappa_i$, where κ_i is the intrinsic decay rate of R_A. The term $\pounds_n[L_{bs}]\rho_{\rm fw}$ describes the effective thermalization noise of the mode $b_{s\circlearrowleft}$ resulting from the *classical coherent* pump. It is given by $\pounds_n[L_{bs}]\rho_{\rm fw} = N_p\mathcal{L}[L_{bs}]\rho_{\rm fw} + N_p\mathcal{L}[L_{bs}^\dagger]\rho_{\rm fw} - M_p\mathcal{L}'[L_{bs}]\rho_{\rm fw} - M_p^*\mathcal{L}'[L_{bs}^\dagger]\rho_{\rm fw}$, where $N_p = \sinh^2(r_p)$, $M_p = e^{i\theta_p}\cosh(r_p)\sinh(r_p)$, and $\mathcal{L}'[o]\rho = 2o\rho o - oo\rho - \rho oo$. This noise can limit the application of the system in the quantum regime.

For achieving single-photon isolation, we can apply a broadband squeezed-vacuum field to cancel the pump-induced noise associated term $\pounds_n[L_{bs}]\rho_{\rm fw}$ [43,44,48,53]. Such broadband squeezed-vacuum field has been realized via optical parametric amplification [58]. In doing so, the mode $a_\circlearrowright$ can couple to the squeezed mode $b_{s\circlearrowleft}$ coherently without additional noise, just as a simple linear resonator system. The squeezed mode is equivalently coupled to a normal vacuum bath and has a decay rate of κ_b.

For the backward-input case, the Hamiltonian reads $\mathcal{H}_{\rm bw}/\hbar = \Delta_a a_\circlearrowleft^\dagger a_\circlearrowleft + i\sqrt{2\kappa_{\rm ex1}}(a_{\rm in}a_\circlearrowleft^\dagger - a_{\rm in}^\dagger a_\circlearrowleft) + \Delta_b^0 b_\circlearrowright^\dagger b_\circlearrowright + J_0(a_\circlearrowleft^\dagger b_\circlearrowright + b_\circlearrowright^\dagger a_\circlearrowleft)$, where $\Delta_b^0 = \omega_b - \omega_{\rm in}$. Comparing the Hamiltonians $\mathcal{H}_{\rm fw}^s$ and $\mathcal{H}_{\rm bw}$, we can see that the intermode detuning and coupling in these two Hamiltonians can be very different due to the directional quantum squeezing. The dynamics of the system is governed by the master equation of two coupling resonators $d\rho_{\rm bw}/dt = -i[\mathcal{H}_{\rm bw}, \rho_{\rm bw}] + \mathcal{L}[L_a]\rho_{\rm bw} + \mathcal{L}[L_b]\rho_{\rm bw}$, where $\rho_{\rm bw}$ is the density matrix of the system, $L_a = \sqrt{\kappa_a} a_{\circlearrowleft}$, and $L_b = \sqrt{\kappa_b} b_{\circlearrowright}$. Note that in this case the squeezed-vacuum field has no influence on the dynamics. Thus, we can attain strong ONR by parametrically pumping the mode $b_{\circlearrowleft}$.

According to the input-output relation [59], for an input field $a_{\rm in}$, we have $a_{\rm out} = a_{\rm in} - \sqrt{2\kappa_{\rm ex1}} a$ and $b_{\rm out} = \sqrt{2\kappa_{\rm ex2}} b$, where $\kappa_{\rm ex2}$ is the external decay rate of R_B. The transmissions are defined as $T_{12/21} = \langle a^\dagger_{\rm out} a_{\rm out}\rangle / \langle a^\dagger_{\rm in} a_{\rm in}\rangle$ and $T_{23} = \langle b^\dagger_{\rm out} b_{\rm out}\rangle / \langle a^\dagger_{\rm in} a_{\rm in}\rangle$, where T_{ij} is the transmission from port i to port j, with i, $j = 1, 2, 3$. Numerically solving the master equations and using $\alpha_{\rm in} \equiv \langle a_{\rm in}\rangle = \sqrt{2\pi P_{\rm in}/\hbar\omega_{\rm in}}$ with the signal power $P_{\rm in}$, we can obtain the steady-state solutions for $\langle a^\dagger_{\rm out} a_{\rm out}\rangle_{\rm ss}$ and $\langle b^\dagger_{\rm out} b_{\rm out}\rangle_{\rm ss}$, and the steady-state transmissions.

We can also analytically derive the transmissions from the Langevin equations of motion. To consider the pump-induced noise, we truncate the Langevin equations to second-order nonlinear terms of operators and obtain

$$\begin{aligned}
da_x/dt &= -(i\Delta_a + \kappa_a) a_x + \sqrt{2\kappa_{\rm ex1}} a_{\rm in} - iJ_x b_x,\\
db_x/dt &= -(i\Delta^x_b + \kappa_b) b_x - iJ_x a_x,\\
d(a^\dagger_x b_x)/dt &= (i\Delta^x_{ab} - \kappa_{ab}) a^\dagger_x b_x + \sqrt{2\kappa_{\rm ex1}} a^\dagger_{\rm in} b_x - iJ_x \Xi,\\
d(b^\dagger_x b_x)/dt &= iJ_x (a^\dagger_x b_x - a_x b^\dagger_x) - 2\kappa_b b^\dagger_x b_x + \Psi_{\rm noise},\\
d(a^\dagger_x a_x)/dt &= -2\kappa_a a^\dagger_x a_x - (iJ_x a^\dagger_x b_x - \sqrt{2\kappa_{\rm ex1}} a_{\rm in} a^\dagger_x + \text{H.c.}),
\end{aligned} \tag{2}$$

where the pump-induced noise $\Psi_{\rm noise} = 2\sinh^2(r_p)\kappa_b$ is present in the forward-input case and plays the role of a thermal bath. In the backward-input case, $\Psi_{\rm noise}$ is absent. We have used $\Delta^x_{ab} = \Delta_a - \Delta^x_b$, $\kappa_{ab} = \kappa_a + \kappa_b$ and $\Xi = a^\dagger_x a_x - b^\dagger_x b_x$. In the calculations, we need to, respectively, replace $a_x, b_x, J_x, \Delta^x_b$ with $a_{\circlearrowright}, b_{s\circlearrowleft}, J_s, \Delta^s_b$ ($a_{\circlearrowleft}, b_{\circlearrowright}, J_0, \Delta^0_b$) for the forward-input (backward-input) case [53]. By solving the Langevin equations and using the input-output relations, we obtain the steady-state transmissions

$$\begin{aligned}
T_{12} &= (J^4_s + 2\zeta_s J^2_s + \Lambda_s)/\mathcal{G}_s + 2\kappa_{\rm ex1}\mathcal{N}_{\rm noise}/|\alpha_{\rm in}|^2,\\
T_{21} &= (J^4_0 + 2\zeta_0 J^2_0 + \Lambda_0)/\mathcal{G}_0, \qquad T_{23} = 4\kappa_{\rm ex1}\kappa_{\rm ex2} J^2_0/\mathcal{G}_0,
\end{aligned} \tag{3}$$

where $\mathcal{N}_{\rm noise} = \kappa_b(\kappa_a + \kappa_b)\sinh^2(r_p) J^2_s/\mathcal{Q}_s$ is the number of noise-related photons, $\mathcal{Q}_s = J^2_s(\kappa_a + \kappa_b)^2 + \kappa_a\kappa_b[(\kappa_a + \kappa_b)^2 + \Delta^{s\,2}_{ab}]$, $\mathcal{G}_x = J^4_x + 2J^2_x(\kappa_a\kappa_b - \Delta_a\Delta^x_b) + (\kappa^2_a + \Delta^2_a)(\kappa^2_b + \Delta^{x\,2}_b)$, $\zeta_x = \kappa_a\kappa_b - 2\kappa_b\kappa_{\rm ex1} - \Delta_a\Delta^x_b$, and $\Lambda_x = [(\kappa_a - 2\kappa_{\rm ex1})^2 + \Delta^2_a](\kappa^2_b + \Delta^{x\,2}_b)$ with $x = \{s, 0\}$. We define the isolation ratio as $\eta = 10\log_{10}(T_{12}/T_{21})$.

By applying the squeezed-vacuum field to cancel the noise $\Psi_{\rm noise}$, the steady-state noise-free transmissions become

$$T^{\rm sv}_{12} = (J^4_s + 2\zeta_s J^2_s + \Lambda_s)/\mathcal{G}_s, \qquad T^{\rm sv}_{21} = T_{21}, \qquad T^{\rm sv}_{23} = T_{23}. \tag{4}$$

$T^{\rm sv}_{12}$ is the limitation of T_{12} for a classical large input $\alpha_{\rm in}$ and also valid for single-photon pulses. Thus, we can achieve ONR in both the classical and quantum regimes. Below, we assume $\Delta_a = \Delta^0_b = \Delta$ and $\kappa_a = \kappa_b = \kappa$.

Next, we will show two different mechanisms to achieve a strong ONR dependence on the bare mode coupling rate J_0. When $J_0 < \kappa$, the two resonators originally have no NMS. We use the pump field to induce the NMS between $a_{\circlearrowright}$ and $b_{s\circlearrowleft}$, namely, the NMS scenario. For $J_0 \gg \kappa$ resulting in the NMS between the bare modes, we use the pump field to significantly shift the resonance frequency of the mode $b_{s\circlearrowleft}$. We call this mechanism the mode resonance shift (MRS) scenario. Under the optimal condition $[(J^2_0 + \kappa^2_i) - (\kappa^2_{\rm ex1} + \Delta^2)]^2 + (2\kappa_i\Delta)^2 \approx 0$, we obtain near-zero T_{21} and thus the maximal isolation ratio

$$\eta_{\rm max} \approx 10\log_{10}\left[\left(1 - \sigma + \frac{2\kappa\mathcal{N}_{\rm noise}}{|\alpha_{\rm in}|^2}\right)\frac{4J^4_0}{\kappa^4_i}\right] \tag{5}$$

at $\Delta = 0$ in the NMS scenario, where $\sigma \approx 4J^2_s\kappa^2/[(J^2_s + \kappa^2)^2 + \kappa^2\Delta^{s\,2}_b]$ and $\kappa \approx \kappa_{\rm ex1}$, or

$$\eta_{\rm max} \approx 10\log_{10}\left[\left(1 + \frac{2\kappa\mathcal{N}_{\rm noise}}{|\alpha_{\rm in}|^2}\right)\frac{J^2_0\kappa^2}{(J^2_0 - \kappa^2)\kappa^2_i}\right] \tag{6}$$

at $\Delta \approx \sqrt{J^2_0 - \kappa^2}$ in the MRS scenario [53].

Our system can realize an optical diode with transmission $T_{12} \gg T_{21}$ even with only the *classical coherent* pump Ω_p. For a weak input signal, e.g., $\alpha_{\rm in}/\sqrt{\kappa} = 0.6$, the transmission T_{12} can be larger than unity, because of the pump-induced noise. When $\alpha_{\rm in}/\sqrt{\kappa} > 3$, corresponding to an input including more than 9 photons within the resonator decay time, the input signal overwhelms the pump-induced noise. In this case, the transmission T_{12} in the classical regime approximates the noise-free transmission $T^{\rm sv}_{12}$ in the quantum regime. Below, we focus on the noise-free case, which is a good approximation of the classical case with a large input signal. In the NMS scenario, we choose $J_0 = 0.99\kappa$ for the optimal condition, such that the transmission $T^{\rm sv}_{21}$ vanishes at $\Delta = 0$. In the forward-input case, the squeezing interaction enhances the coupling strength J_s to much larger than the system decay rates and leads to a large NMS; see Fig. 2(a). Therefore, we obtain $T^{\rm sv}_{12} \approx 83.1\%$ and $T^{\rm sv}_{21} \approx 0$ at $\Delta = 0$, corresponding to an isolation ratio $\eta^{\rm sv} = 10\log_{10}(T^{\rm sv}_{12}/T^{\rm sv}_{21}) \approx 85.1$ dB, insertion loss $L^{\rm sv} = -10\log_{10}(T^{\rm sv}_{12}) \approx 0.80$ dB. In the MRS scenario, we take $J_0 = 2.8\kappa$, for example. The transmission spectrum

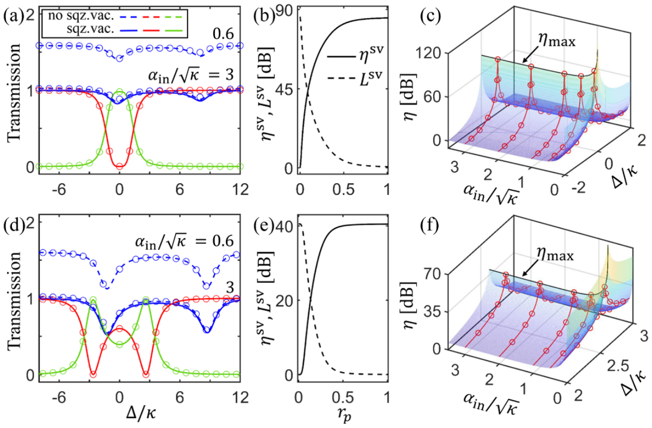

FIG. 2. (a) and (d) Steady-state transmission versus the detuning Δ. Dashed curves and open circles are for the analytical and numerical transmissions T_{12} (blue), T_{21} (red), and T_{23} (green), respectively. Solid curves are for the corresponding analytical transmission of T_{ij}^{sv}. (b) and (e) Isolation ratio and insertion loss versus r_p. (c) and (f) Isolation ratio η versus α_{in} and Δ (3D surface). Red curves and open circles are for analytical and numerical results. Black curves are for the maximal isolation ratio η_{max} given by Eqs. (5), (6). (a),(b), and (c) for the NMS scenario ($J_0/\kappa = 0.99$); (d),(e), and (f) for the MRS scenario ($J_0/\kappa = 2.8$). Other parameters are $\kappa_{ex1,2}/\kappa = 0.99$; in (a) and (c) $\Delta_p^b/\kappa = 10.3$, $\Omega_p/\kappa = 10$, yielding $r_p \sim 1.05$; in (d) and (f) $\Delta_p^b/\kappa = 15$, $\Omega_p/\kappa = 13$, yielding $r_p \sim 0.66$; in (b) $\Delta = 0$ and $\Delta_p^b/\kappa = 10\sinh(r_p)$; in (e) $\Delta/\kappa = 2.62$ and $\Delta_p^b/\kappa = 30\sinh(r_p)$.

splits in the backward-input case. In the forward-input case, the resonance frequency of the squeezed mode is shifted and thus detuned from the mode $a_{\circlearrowright}$. The transmission spectrum is shifted with respect to the backward-input transmission, see Fig. 2(d). As a result, we attain $T_{12}^{sv} \approx 92.8\%$ and $T_{21}^{sv} \approx 0$ at $\Delta/\kappa = 2.62$, corresponding to $\eta^{sv} \approx 40.3$ dB, $L^{sv} \approx 0.32$ dB. The isolation ratio and the insertion loss improve with r_p and reach stable values when $r_p > 0.6$, see Figs. 2(b), 2(e). We also study the isolation ratios η versus the detuning and the input, see Figs. 2(c), 2(f). When $\alpha_{in}/\sqrt{\kappa} > 1$, η already approaches the noise-free case. In this, the bandwidth for $\eta \geq 20$ dB is about 0.86κ (0.21κ) for the NMS (MRS) scenario. In our numerical calculations, we truncate the Hilbert space of the resonator modes to high Fock states such that the numerical transmission and the isolation ratio reach high accuracies. The analytical and numerical results are in excellent agreement.

Similar to a commercial circulator, our proposed system can also function as a quasicirculator with two inputs and three outputs, allowing photon flow along the direction $1 \to 2 \to 3$ [60], see Figs. 2(a), 2(d). Here, we focus on the fidelity and the insertion loss. To evaluate the quasicirculator performance, we calculate the average fidelity as $\mathcal{F} = \mathrm{Tr}[\tilde{T}T_{id}^T]/\mathrm{Tr}[T_{id}T_{id}^T]$ [19,34], where T_{id}^T is the transmission matrix for an ideal three-port quasicirculator [60], and $\tilde{T} = T_{ij}/\Upsilon_i$, with $\Upsilon_i = \sum_j T_{ij}$. We define the average insertion loss as $\tilde{L} = -10\log[(T_{12} + T_{23})/2]$. The transmissions T_{12} and T_{21} are the same as the diode. For an input $\alpha_{in}/\sqrt{\kappa} > 3$, the pump-induced noise is negligible. In the NMS scenario, we achieve $T_{23} \approx 98.0\%$ at $\Delta = 0$, corresponding to $\tilde{L} \approx 0.43$ dB. We also obtain a similar performance in the MRS scenario with $T_{23} \approx 98.0\%$ at $\Delta/\kappa = 2.62$, corresponding to $\tilde{L} \approx 0.20$ dB. In both scenarios, we have $\mathcal{F} \approx 1$.

Our system can work as a single-photon quasicirculator when the squeezing-vacuum field is applied to cancel the noise term. We evaluate its performance for a single-photon wave packet input to ports 1 and 2 simultaneously by solving a quantum cascaded system [61–63] (also Supplemental Material [53]). We consider a Gaussian-like single-photon pulse with duration $2\pi \times 6\kappa^{-1}$. In comparison with the case without the squeezed-vacuum field, the performance of our quasicirculator only slightly decreases. The fidelity is still very high, $\mathcal{F} \geq 98.7\%$. The insertion loss remains unchanged due to the large bandwidth in the NMS scenario. In comparison, it reduces to $\tilde{L} \approx 0.26$ dB at $\Delta/\kappa = 2.62$ in the MRS scenario. Therefore, our diode and quasicirculator can work in both the classical and quantum regimes.

When the pump laser with power P_p is present, corresponding to "on" (absent, corresponding to "off"), our device can switch on and off the transmission of a stronger signal laser from T_{12}^{on} to T_{12}^{off} according to Eq. (3), implying an all-optical nonreciprocal transistor. As the crucial role of electronic transistor in electric computers, optical transistors are essential for optical information processing [64–67]. We define the gain of the transistor as $G = P_{in}\Delta T/P_p$, with $\Delta T = T_{12}^{on} - T_{12}^{off}$ [64]. The gain increases linearly with the signal power. When we fix the pump strength, e.g., $\Omega_p/\kappa = 10$, in the NMS scenario, the gain of the transistor can reach $G > 1$ $(G > 100)$ when $|\alpha_{in}|^2/\kappa > 6.1 \times 10^7$ $(|\alpha_{in}|^2/\kappa > 6.1 \times 10^9)$, see Fig. 3(a). In the MRS scenario, we can obtain the same gain $G > 1$ $(G > 100)$ by taking $\Omega_p/\kappa = 13$ and applying a slightly larger pump power $|\alpha_{in}|^2/\kappa > 9.2 \times 10^7$

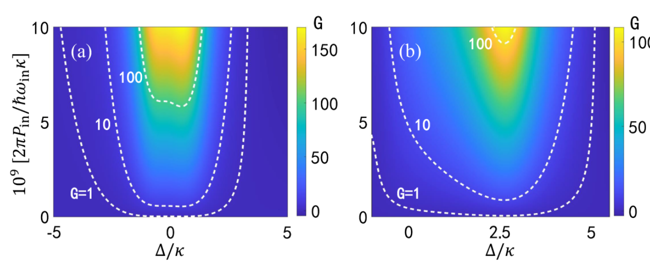

FIG. 3. Gain of the transistor versus detuning Δ and P_{in}. (a) The NMS scenario with $J_0/\kappa = 0.99$, $\Delta_p^b/\kappa = 10.3$, $\Omega_p/\kappa = 10$. (b) The MRS scenario with $J_0/\kappa = 2.8$, $\Delta_p^b/\kappa = 15$, $\Omega_p/\kappa = 13$. Other parameters are $\kappa_{ex1,2}/\kappa = 0.99$, $g/\kappa = 10^{-3}$.

($|\alpha_{\rm in}|^2/\kappa > 9.2\times 10^9$), see Fig. 3(b). Unlike the forward-input case, the transmission T_{21} in the backward-input case is independent of the pump power and always vanishingly small. Clearly, our optical transistor is nonreciprocal.

Lithium-niobate-based microring resonators provide an excellent platform for our proposal, thanks to their large $\chi^{(2)}$ [68–70] and high optical quality factors up to $Q\sim 10^7$ [71,72]. Assuming an experimentally available intrinsic quality factor $Q_i = 8\times 10^6$, the resonance frequency of the signal field $\omega_{a/b}/2\pi = 193.4$ THz and the pump field frequency $\omega_p \approx 2\omega_a$ for the resonators, we obtain the intrinsic loss rate $\kappa_i/2\pi = 24.2$ MHz. By choosing an experimentally available gap [73], we can select feasible values: $\kappa_{\rm ex1,2}\approx 2\pi\times 2.40$ GHz, $\kappa\approx 2\pi\times 2.42$ GHz, and $J_0 = 0.99\kappa \approx 2\pi\times 2.40$ GHz in the NMS scenario ($J_0 = 2.8\kappa\approx 2\pi\times 6.78$ GHz in the MRS scenario). Hence, the nonreciprocal bandwidth for $\eta\geq 20$ dB can reach $0.86\kappa/2\pi\approx 2.08$ GHz around $\Delta = 0$ (or $0.21\kappa/2\pi\approx 0.51$ GHz around $\Delta = 2.62\kappa$). The power of a pump field is given by $P_p = \hbar\omega_p\kappa_p^2\Omega_p^2/(16\pi g^2\kappa_{\rm ex2}^p)$ [53], where κ_p and $\kappa_{\rm ex2}^p$ are, respectively, the total and external decay rates of the mode $c_{\circlearrowleft}$, and g is the nonlinear single-photon coupling strength. The rate of $g/2\pi = 2.35$ MHz is available for lithium-niobate-based microresonators [74]. The pump power $P_p\approx 16.6$ mW (or 28.0 mW) yields to $\Omega_p/\kappa = 10$ (or 13). At the detuning $\Delta/\kappa = 0$ (or 2.62), we can induce an optical transistor with $G > 1$ for a signal power $P_{\rm in}\approx 18.9$ mW in the NMS scenario (or 28.5 mW in the MRS scenario). Because of inevitable imperfections in fabrication, it is not easy to precisely meet the optimal condition and the parameter relationships $\Delta_a = \Delta_b^0$ and $\kappa_a = \kappa_b$. A small derivation of these conditions in fabrication may cause a slight reduction in the performance, particularly the isolation ratio of the nonreciprocal device.

We have proposed a squeezing-based scheme to realize a chip-compatible magnetic-free ONR, including an optical diode, a quasicirculator and a nonreciprocal optical transistor. The optical diode and circulator can work *in the classical regime under a coherent pump and also in the quantum regime when a squeezed-vacuum field is applied*. In particular, our work proposed the nonreciprocal optical transistor switching a strong signal with a weak control field. Such unconventional transistor cannot be realized in the configuration of Ref. [41] because a strong signal will cause NMS for the pump field. Our protocol paves a way for realizing on-chip all-optical nonreciprocal devices.

This work was supported by the National Key R&D Program of China (Grants No. 2017YFA0303703, No. 2019YFA0308700), the National Natural Science Foundation of China (Grants No. 11874212, No. 11890704), the Program for Innovative Talents and Teams in Jiangsu (Grant No. JSSCTD202138), and the Excellent Research Program of Nanjing University (Grant No. ZYJH002). F. N. is supported by the Nippon Telegraph and Telephone Corporation (NTT) Research, the Japan Science and Technology Agency (JST) [via the Quantum Leap Flagship Program (Q-LEAP), the Moonshot R&D Grant No. JPMJMS2061, and the Centers of Research Excellence in Science and Technology (CREST) Grant No. JPMJCR1676], the Japan Society for the Promotion of Science (JSPS) [via the Grants-in-Aid for Scientific Research (KAKENHI) Grant No. JP20H00134 and the JSPS-RFBR Grant No. JPJSBP120194828], the Army Research Office (ARO) (Grant No. W911NF-18-1-0358), the Asian Office of Aerospace Research and Development (AOARD) (via Grant No. FA2386-20-1-4069), and the Foundational Questions Institute Fund (FQXi) via Grant No. FQXi-IAF19-06. We thank the High Performance Computing Center of Nanjing University for doing the numerical calculations on its blade cluster system.

*keyu.xia@nju.edu.cn

[1] T. Goto, A. V. Dorofeenko, A. M. Merzlikin, A. V. Baryshev, A. P. Vinogradov, M. Inoue, A. A. Lisyansky, and A. B. Granovsky, Optical Tamm States in One-Dimensional Magnetophotonic Structures, Phys. Rev. Lett. **101**, 113902 (2008).

[2] Z. Guo, F. Wu, C. Xue, H. Jiang, Y. Sun, Y. Li, and H. Chen, Significant enhancement of magneto-optical effect in one-dimensional photonic crystals with a magnetized epsilon-near-zero defect, J. Appl. Phys. **124**, 103104 (2018).

[3] L. Fan, J. Wang, L. T. Varghese, H. Shen, B. Niu, Y. Xuan, A. M. Weiner, and M. Qi, An all-silicon passive optical diode, Science **335**, 447 (2012).

[4] B. Peng, Ş. K. Özdemir, F. Lei, F. Monifi, M. Gianfreda, G. L. Long, S. Fan, F. Nori, C. M. Bender, and L. Yang, Parity-time-symmetric whispering-gallery microcavities, Nat. Phys. **10**, 394 (2014).

[5] L. Chang, X. Jiang, S. Hua, C. Yang, J. Wen, L. Jiang, G. Li, G. Wang, and M. Xiao, Parity-time symmetry and variable optical isolation in active-passive-coupled microresonators, Nat. Photonics **8**, 524 (2014).

[6] Y. Shi, Z. Yu, and S. Fan, Limitations of nonlinear optical isolators due to dynamic reciprocity, Nat. Photonics **9**, 388 (2015).

[7] S. Hua, J. Wen, X. Jiang, Q. Hua, L. Jiang, and M. Xiao, Demonstration of a chip-based optical isolator with parametric amplification, Nat. Commun. **7**, 13657 (2016).

[8] B. He, L. Yang, X. Jiang, and M. Xiao, Transmission Nonreciprocity in a Mutually Coupled Circulating Structure, Phys. Rev. Lett. **120**, 203904 (2018).

[9] L. D. Bino, J. M. Silver, M. T. M. Woodley, S. L. Stebbings, X. Zhao, and P. Del'Haye, Microresonator isolators and circulators based on the intrinsic nonreciprocity of the Kerr effect, Optica **5**, 279 (2018).

[10] K. Y. Yang, J. Skarda, M. Cotrufo, A. Dutt, G. H. Ahn, M. Sawaby, D. Vercruysse, A. Arbabian, S. Fan, A. Alù, and J. Vučković, Inverse-designed non-reciprocal pulse router for chip-based lidar, Nat. Photonics **14**, 369 (2020).

[11] L. Tang, J. Tang, H. Wu, J. Zhang, M. Xiao, and K. Xia, Broad-intensity-range optical nonreciprocity based on

feedback-induced Kerr nonlinearity, Photonics Res. **9**, 1218 (2021).
[12] H. Lira, Z. Yu, S. Fan, and M. Lipson, Electrically Driven Nonreciprocity Induced by Interband Photonic Transition on a Silicon Chip, Phys. Rev. Lett. **109**, 033901 (2012).
[13] N. A. Estep, D. L. Sounas, J. Soric, and A. Alù, Magnetic-free non-reciprocity and isolation based on parametrically modulated coupled-resonator loops, Nat. Phys. **10**, 923 (2014).
[14] D. L. Sounas and A. Alù, Non-reciprocal photonics based on time modulation, Nat. Photonics **11**, 774 (2017).
[15] K. Xia, G. Lu, G. Lin, Y. Cheng, Y. Niu, S. Gong, and J. Twamley, Reversible nonmagnetic single-photon isolation using unbalanced quantum coupling, Phys. Rev. A **90**, 043802 (2014).
[16] K. Y. Bliokh, D. Smirnova, and F. Nori, Quantum spin Hall effect of light, Science **348**, 1448 (2015).
[17] K. Y. Bliokh and F. Nori, Transverse and longitudinal angular momenta of light, Phys. Rep. **592**, 1 (2015).
[18] K. Y. Bliokh, F. J. Rodríguez-Fortuño, F. Nori, and A. V. Zayats, Spin-orbit interactions of light, Nat. Photonics **9**, 796 (2015).
[19] M. Scheucher, A. Hilico, E. Will, J. Volz, and A. Rauschenbeutel, Quantum optical circulator controlled by a single chirally coupled atom, Science **354**, 1577 (2016).
[20] P. Lodahl, S. Mahmoodian, S. Stobbe, A. Rauschenbeutel, P. Schneeweiss, J. Volz, H. Pichler, and P. Zoller, Chiral quantum optics, Nature (London) **541**, 473 (2017).
[21] K. Y. Bliokh, D. Leykam, M. Lein, and F. Nori, Topological non-Hermitian origin of surface Maxwell waves, Nat. Commun. **10**, 580 (2019).
[22] L. Tang, J. Tang, W. Zhang, G. Lu, H. Zhang, Y. Zhang, K. Xia, and M. Xiao, On-chip chiral single-photon interface: Isolation and unidirectional emission, Phys. Rev. A **99**, 043833 (2019).
[23] S. Guddala, Y. Kawaguchi, F. Komissarenko, S. Kiriushechkina, A. Vakulenko, K. Chen, A. Alù, V. M. Menon, and A. B. Khanikaev, All-optical nonreciprocity due to valley polarization pumping in transition metal dichalcogenides, Nat. Commun. **12**, 3746 (2021).
[24] S. Manipatruni, J. T. Robinson, and M. Lipson, Optical Nonreciprocity in Optomechanical Structures, Phys. Rev. Lett. **102**, 213903 (2009).
[25] Z. Shen, Y.-L. Zhang, Y. Chen, C.-L. Zou, Y.-F. Xiao, X.-B. Zou, F.-W. Sun, G.-C. Guo, and C.-H. Dong, Experimental realization of optomechanically induced non-reciprocity, Nat. Photonics **10**, 657 (2016).
[26] Z. Shen, Y.-L. Zhang, Y. Chen, F.-W. Sun, X.-B. Zou, G.-C. Guo, C.-L. Zou, and C.-H. Dong, Reconfigurable optomechanical circulator and directional amplifier, Nat. Commun. **9**, 1797 (2018).
[27] D.-W. Wang, H.-T. Zhou, M.-J. Guo, J.-X. Zhang, J. Evers, and S.-Y. Zhu, Optical Diode Made from a Moving Photonic Crystal, Phys. Rev. Lett. **110**, 093901 (2013).
[28] S. A. R. Horsley, J.-H. Wu, M. Artoni, and G. C. La Rocca, Optical Nonreciprocity of Cold Atom Bragg Mirrors in Motion, Phys. Rev. Lett. **110**, 223602 (2013).
[29] J.-H. Wu, M. Artoni, and G. C. La Rocca, Non-Hermitian Degeneracies and Unidirectional Reflectionless Atomic Lattices, Phys. Rev. Lett. **113**, 123004 (2014).
[30] X. Lu, W. Cao, W. Yi, H. Shen, and Y. Xiao, Nonreciprocity and Quantum Correlations of Light Transport in Hot Atoms via Reservoir Engineering, Phys. Rev. Lett. **126**, 223603 (2021).
[31] S. Maayani, R. Dahan, Y. Kligerman, E. Moses, A. U. Hassan, H. Jing, F. Nori, D. N. Christodoulides, and T. Carmon, Flying couplers above spinning resonators generate irreversible refraction, Nature (London) **558**, 569 (2018).
[32] R. Huang, A. Miranowicz, J.-Q. Liao, F. Nori, and H. Jing, Nonreciprocal Photon Blockade, Phys. Rev. Lett. **121**, 153601 (2018).
[33] Y.-F. Jiao, S.-D. Zhang, Y.-L. Zhang, A. Miranowicz, L.-M. Kuang, and H. Jing, Nonreciprocal Optomechanical Entanglement Against Backscattering Losses, Phys. Rev. Lett. **125**, 143605 (2020).
[34] K. Xia, F. Nori, and M. Xiao, Cavity-Free Optical Isolators and Circulators using a Chiral Cross-Kerr Nonlinearity, Phys. Rev. Lett. **121**, 203602 (2018).
[35] S. Zhang, Y. Hu, G. Lin, Y. Niu, K. Xia, J. Gong, and S. Gong, Thermal-motion-induced non-reciprocal quantum optical system, Nat. Photonics **12**, 744 (2018).
[36] Y. Hu, S. Zhang, Y. Qi, G. Lin, Y. Niu, and S. Gong, Multiwavelength Magnetic-Free Optical Isolator by Optical Pumping in Warm Atoms, Phys. Rev. Applied **12**, 054004 (2019).
[37] P. Yang, X. Xia, H. He, S. Li, X. Han, P. Zhang, G. Li, P. Zhang, J. Xu, Y. Yang, and T. Zhang, Realization of Nonlinear Optical Nonreciprocity on a Few-Photon Level based on Atoms Strongly Coupled to an Asymmetric Cavity, Phys. Rev. Lett. **123**, 233604 (2019).
[38] C. Liang, B. Liu, A.-N. Xu, X. Wen, C. Lu, K. Xia, M. K. Tey, Y.-C. Liu, and L. You, Collision-Induced Broadband Optical Nonreciprocity, Phys. Rev. Lett. **125**, 123901 (2020).
[39] M.-X. Dong, K.-Y. Xia, W.-H. Zhang, Y.-C. Yu, Y.-H. Ye, E.-Z. Li, L. Zeng, D.-S. Ding, B.-S. Shi, G.-C. Guo, and F. Nori, All-optical reversible single-photon isolation at room temperature, Sci. Adv. **7**, eabe8924 (2021).
[40] Y. Hu, Y. Qi, Y. You, S. Zhang, G. Lin, X. Li, J. Gong, S. Gong, and Y. Niu, Passive Nonlinear Optical Isolators Bypassing Dynamic Reciprocity, Phys. Rev. Applied **16**, 014046 (2021).
[41] X. Guo, C.-L. Zou, H. Jung, and H. X. Tang, On-Chip Strong Coupling and Efficient Frequency Conversion between Telecom and Visible Optical Modes, Phys. Rev. Lett. **117**, 123902 (2016).
[42] J.-Q. Wang, Y.-H. Yang, M. Li, X.-X. Hu, J. B. Surya, X.-B. Xu, C.-H. Dong, G.-C. Guo, H. X. Tang, and C.-L. Zou, Efficient Frequency Conversion in a Degenerate $\chi^{(2)}$ Microresonator, Phys. Rev. Lett. **126**, 133601 (2021).
[43] X.-Y. Lü, Y. Wu, J. R. Johansson, H. Jing, J. Zhang, and F. Nori, Squeezed Optomechanics with Phase-Matched Amplification and Dissipation, Phys. Rev. Lett. **114**, 093602 (2015).
[44] W. Qin, A. Miranowicz, P.-B. Li, X.-Y. Lü, J. Q. You, and F. Nori, Exponentially Enhanced Light-Matter Interaction, Cooperativities, and Steady-State Entanglement using Parametric Amplification, Phys. Rev. Lett. **120**, 093601 (2018).

[45] C. Leroux, L. C. G. Govia, and A. A. Clerk, Enhancing Cavity Quantum Electrodynamics via Antisqueezing: Synthetic Ultrastrong Coupling, Phys. Rev. Lett. **120**, 093602 (2018).

[46] W. Ge, B. C. Sawyer, J. W. Britton, K. Jacobs, J. J. Bollinger, and M. Foss-Feig, Trapped Ion Quantum Information Processing with Squeezed Phonons, Phys. Rev. Lett. **122**, 030501 (2019).

[47] W. Zhao, S.-D. Zhang, A. Miranowicz, and H. Jing, Weak-force sensing with squeezed optomechanics, Sci. China Phys. Mech. Astron. **63**, 224211 (2020).

[48] W. Qin, V. Macrì, A. Miranowicz, S. Savasta, and F. Nori, Emission of photon pairs by mechanical stimulation of the squeezed vacuum, Phys. Rev. A **100**, 062501 (2019).

[49] C. J. Zhu, L. L. Ping, Y. P. Yang, and G. S. Agarwal, Squeezed Light Induced Symmetry Breaking Superradiant Phase Transition, Phys. Rev. Lett. **124**, 073602 (2020).

[50] Y.-H. Chen, W. Qin, X. Wang, A. Miranowicz, and F. Nori, Shortcuts to Adiabaticity for the Quantum Rabi Model: Efficient Generation of Giant Entangled Cat States via Parametric Amplification, Phys. Rev. Lett. **126**, 023602 (2021).

[51] S. C. Burd, R. Srinivas, H. M. Knaack, W. Ge, A. C. Wilson, D. J. Wineland, D. Leibfried, J. J. Bollinger, D. T. C. Allcock, and D. H. Slichter, Quantum amplification of boson-mediated interactions, Nat. Phys. **17**, 898 (2021).

[52] W. Qin, A. Miranowicz, H. Jing, and F. Nori, Generating Long-Lived Macroscopically Distinct Superposition States in Atomic Ensembles, Phys. Rev. Lett. **127**, 093602 (2021).

[53] See Supplemental Material http://link.aps.org/supplemental/10.1103/PhysRevLett.128.083604 for more technical details of our system and methods, which includes Refs. [54,55].

[54] K. Xia, F. Jelezko, and J. Twamley, Quantum routing of single optical photons with a superconducting flux qubit, Phys. Rev. A **97**, 052315 (2018).

[55] A. H. Kiilerich and K. Mølmer, Input-Output Theory with Quantum Pulses, Phys. Rev. Lett. **123**, 123604 (2019).

[56] M. O. Scully and M. S. Zubairy, *Quantum Optics* (Cambridge University Press, Cambridge, England, 1997).

[57] G. S. Agarwal, *Quantum Optics* (Cambridge University Press, Cambridge, England, 2012).

[58] T. Kashiwazaki, N. Takanashi, T. Yamashima, T. Kazama, K. Enbutsu, R. Kasahara, T. Umeki, and A. Furusawa, Continuous-wave 6-dB-squeezed light with 2.5-THz-bandwidth from single-mode PPLN waveguide, APL Photonics **5**, 036104 (2020).

[59] C. W. Gardiner and M. J. Collett, Input and output in damped quantum systems: Quantum stochastic differential equations and the master equation, Phys. Rev. A **31**, 3761 (1985).

[60] S. V. Kutsaev, A. Krasnok, S. N. Romanenko, A. Y. Smirnov, K. Taletski, and V. P. Yakovlev, Up-and-coming advances in optical and microwave nonreciprocity: From classical to quantum realm, Adv. Photonics Res. **2**, 2000104 (2021).

[61] C. W. Gardiner, Driving a Quantum System with the Output Field from Another Driven Quantum System, Phys. Rev. Lett. **70**, 2269 (1993).

[62] H. J. Carmichael, Quantum Trajectory Theory for Cascaded Open Systems, Phys. Rev. Lett. **70**, 2273 (1993).

[63] K. Stannigel, P. Rabl, and P. Zoller, Driven-dissipative preparation of entangled states in cascaded quantum-optical networks, New J. Phys. **14**, 063014 (2012).

[64] S. Sun, H. Kim, Z. Luo, G. S. Solomon, and E. Waks, A single-photon switch and transistor enabled by a solid-state quantum memory, Science **361**, 57 (2018).

[65] W. Chen, K. M. Beck, R. Bücker, M. Gullans, M. D. Lukin, H. Tanji-Suzuki, and V. Vuletić, All-optical switch and transistor gated by one stored photon, Science **341**, 768 (2013).

[66] J. Hwang, M. Pototschnig, R. Lettow, G. Zumofen, A. Renn, S. Götzinger, and V. Sandoghdar, A single-molecule optical transistor, Nature (London) **460**, 76 (2009).

[67] D. Ballarini, M. De Giorgi, E. Cancellieri, R. Houdré, E. Giacobino, R. Cingolani, A. Bramati, G. Gigli, and D. Sanvitto, All-optical polariton transistor, Nat. Commun. **4**, 1778 (2013).

[68] C. Wang, X. Xiong, N. Andrade, V. Venkataraman, X.-F. Ren, G.-C. Guo, and M. Lončar, Second harmonic generation in nano-structured thin-film lithium niobate waveguides, Opt. Express **25**, 6963 (2017).

[69] M. Wang, N. Yao, R. Wu, Z. Fang, S. Lv, J. Zhang, J. Lin, W. Fang, and Y. Cheng, Strong nonlinear optics in on-chip coupled lithium niobate microdisk photonic molecules, New J. Phys. **22**, 073030 (2020).

[70] Z. Ma, J.-Y. Chen, Z. Li, C. Tang, Y. M. Sua, H. Fan, and Y.-P. Huang, Ultrabright Quantum Photon Sources on Chip, Phys. Rev. Lett. **125**, 263602 (2020).

[71] M. Zhang, C. Wang, R. Cheng, A. Shams-Ansari, and M. Lončar, Monolithic ultra-high-Q lithium niobate microring resonator, Optica **4**, 1536 (2017).

[72] B. Desiatov, A. Shams-Ansari, M. Zhang, C. Wang, and M. Lončar, Ultra-low-loss integrated visible photonics using thin-film lithium niobate, Optica **6**, 380 (2019).

[73] Z. Tian, P. Zhang, and X.-W. Chen, Static Hybrid Quantum Nodes: Toward Perfect State Transfer on a Photonic Chip, Phys. Rev. Applied **15**, 054043 (2021).

[74] J. Lu, M. Li, C.-L. Zou, A. A. Sayem, and H. X. Tang, Toward 1% single-photon anharmonicity with periodically poled lithium niobate microring resonators, Optica **7**, 1654 (2020).